Computer-aided Product Design with Performance-Tailored Mesostructures

Yong Chen and Shanglong Wang

University of Southern California, {yongchen,shanglow}@usc.edu

ABSTRACT

Motivated by the design and manufacturing of customized cushions for debilitated patients, we propose the idea of performance-tailored mesostructures which can change or adapt their design performance based on given requirements. Our goal is to develop a CAD tool with the capability of specifying heterogeneous material properties in a product component such that a designer can design the component with better performance. Based on the object oriented programming paradigm, we first define a performance-tailored mesostructure and its properties. We then demonstrate an approach of building discipline-specific performance models for such mesostructures. For a product component design, we present a performance-tailored mesostructure design method based on a hierarchical design framework. A CAD system based on the proposed design framework is being developed which can generate CAD models with performance-tailored mesostructures. The generated CAD models can then be fabricated by a layer-based rapid manufacturing system. Several experimental examples are given to demonstrate the capability of our method.

$$E_y = E_z >> E_{x1} > E_{x2} > E_{x3} > E_{x4}$$
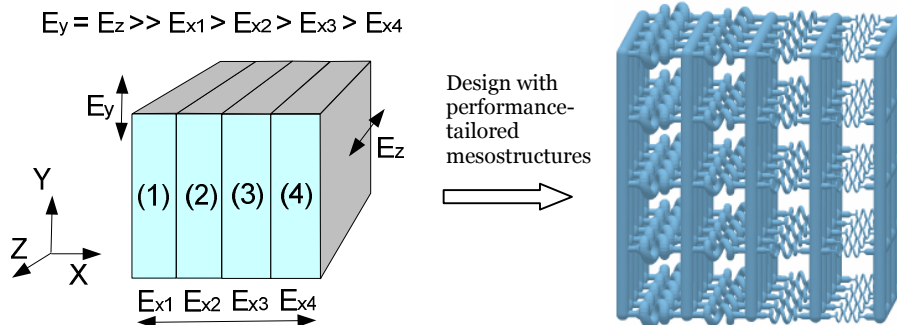
Fig. 1: An illustration of the performance-tailored mesostructures to achieve heterogeneous material properties. Suppose the designer specifies a simple cube design (left), in which, the material's Young's modulus in *Y* and *Z* axes is much bigger than that in *X* axis; further, the material's Young's modulus needs to decrease along *X* axis. Based on the desired material properties, a CAD model generated by our approach for the cube design is shown in the figure (right).

1. INTRODUCTION

Our research is motivated by the pressure sore problem that is quite common among debilitated patients, especially those who have spinal cord injury and other neurological impairments. Pressure sores tend to occur over bony projection areas where pressure is concentrated. The essential reason for the pressure sore is that the skin has a rich

blood supply that delivers oxygen to all its layers. If the blood supply is cut off for more than 2 or 3 hours, the skin dies, beginning at its outer layer. The dead skin breaks down and forms an open sore or ulcer. Once the skin is broken, bacteria may enter the opening and cause an infection [1]. Therefore the risk of developing pressure sores is quite high for those patients who lost their capability of shifting positions when using a wheelchair. The management of pressure sores is very costly and labor-intensive. Therefore the prevention of pressure sores is essential for the patients.

In many cases, an optimal cushion design for the wheelchair is the most effective means of preventing pressure sores. For a long period of time, people have been using soft materials in the cushion design to reduce pressures. For example, comparing the usage of a rigid flat surface (e.g. E=10,000 kPa) and a firm foam cushion (e.g. E=100 kPa) as the contact surface, the foam cushion can help to significantly reduce the maximum internal tissue stresses. Many different types of soft materials have been used in the cushion design. However, the cushion design based on soft materials such as air-cell or gel-pad can only reduce and equalize all contact pressures. The pressure over bony projection areas may still block the blood supply. Therefore, the pressure sores may still happen to those debilitated patients.

A more effective way to reduce the pressure sore problem is based on "pressure redistribution" [2]. That is, a cushion designer can repartition the contact surface and selectively increase or decrease the contact pressure at specific sites or regions. In a sitting position as shown in Figure 2 (left), the posterior thigh region, marked as (1), is less prone to pressure sores than the trochanter area, marked as (2). This is become the distribution of blood vessels and tissue structures in these regions are different. Therefore, an optimized scheme in the cushion design is to develop a cushion such that it can shift the pressure from the areas that can't handle the pressure to the areas that can. The risk of developing pressure sores is greatly reduced by such a cushion that can minimize the intra-tissue stress in the critical areas that are prone to pressure sores.
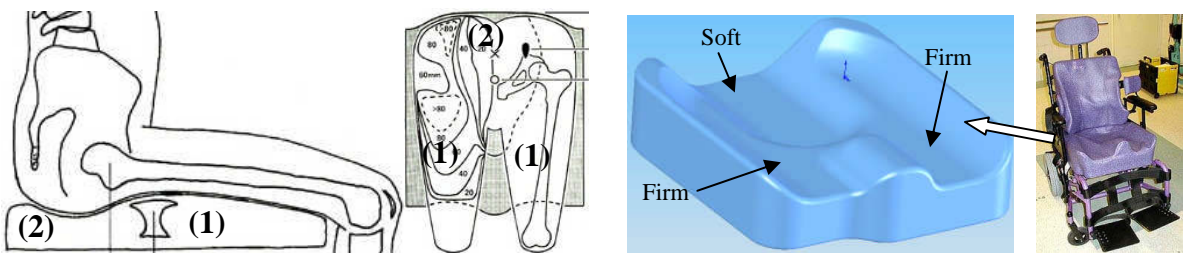
Fig. 2: Pressure redistribution in cushion design (provided by *Richard Pasillas* at *Cushmaker.com*).

An ideal CAD tool, therefore, is to allow a cushion designer to repartition the shape of a seat cushion into small regions and specify the firmness of each region based on the desired pressure distribution. An example from *Richard Pasillas* at *Cushmaker.com* is shown in Figure 2 – (right). Currently foams with a variety of density are manually cut into multiple layers and glue together to fit a patient's custom contour. However, designing such an adequate cushion has been a trial-and-error process since many factors govern the cushion's effectiveness for pressure relief. In addition, the limited selection of foams or plastics can limit the designer's capability in designing such a cushion. Therefore, it is quite costly for a patient to buy a truly customized cushion for his/her wheelchair.

Layer-based additive manufacturing processes, such as stereolithgraphy (SLA) and selective laser sintering (SLS), have been used for prototyping for nearly twenty years (rapid prototyping). A main benefit of a rapid prototyping process is its ability to build arbitrary geometries without tooling. Parts with complex geometries can be manufactured by these processes without cost penalty. In recent year, layer manufacturing processes have been used as a direct manufacturing approach (rapid manufacturing) for aerospace and medical applications. Rapid manufacturing is expected to have a big impact to the future product design and manufacturing [3]. We believe the design and manufacturing of customized cushions can greatly benefit from rapid manufacturing since each cushion is unique based on a patient's specific needs.

In this paper we present a novel product design method based on an idea of performance-tailored mesostructures for achieving heterogeneous material properties that are common in many applications. An illustrative example is shown in Figure 1. In our method, the designer only needs to specify the performance required in each region of a product

component. Our approach and related algorithms will select a suitable mesostructure from a mesostructure library for each region; further we will tailor the geometric parameters of each mesostructure to match the specified performance. Finally based on the common boundaries specified in the structure library, we automatically connect all the mesostructures together to generate a valid CAD model for rapid manufacturing systems. As illustrated in Figure 1, the CAD model generated by our approach fully utilizes the geometric capability of rapid manufacturing processes. The work is part of an effort in developing a CAD tool that gives the cushion designers the most flexibility in designing customized cushions to reduce the possibility of pressure sore.

The central contributions of this paper are the definition of a performance-tailored mesostructure and related design method for an optimal component design. The reminder of the paper is organized in the following way. In Section 2, we define the performance-tailored mesostructure and present the basic idea of using it to achieve heterogeneous material properties. Section 3 illustrates the approach of building functional performance models for a performance-tailored mesostructure library. In Section 4, a hierarchical design framework is presented to integrate the performance-tailored mesostructure with the functional models in the component level. Section 5 summaries our efforts in developing a CAD tool based on the design framework. Two examples are also given to illustrate the capability of our testbed. Finally, conclusions are drawn in Section 6.

2. HETEROGENEOUS MATERIAL PROPERTIES BASED ON MESOSTRUCTURES

We are interested in the design of a product component. In this paper, a mesostructure refers to the geometric arrangement of materials within a unit cell on a scale that is insignificant compared to the scale of the component. The characteristic length of a mesostructure is in the range of 0.1 to 10mm for layer-based rapid manufacturing processes [4]. If a component is solid, its behavior depends on the part geometry and the material property; however, if mesostructures are used in the component, its behavior will also depend on the configuration of the mesostructures. For example, polyhedron, such as tetrahedron and octahedron, are popular mesostructures [5, 6]. An example of applying a polyhedron in a component is shown in Figure 3 (top) [7]. In addition to the simple polyhedron, researchers in the field of material design have presented various meso/micro-structures for different design purposes. For example, Sigmund [8] presented a micro-structure to get material behavior similar to a rubber band. An example of applying Sigmund's mesostructure in a component design is shown in Figure 3 (bottom) [9].
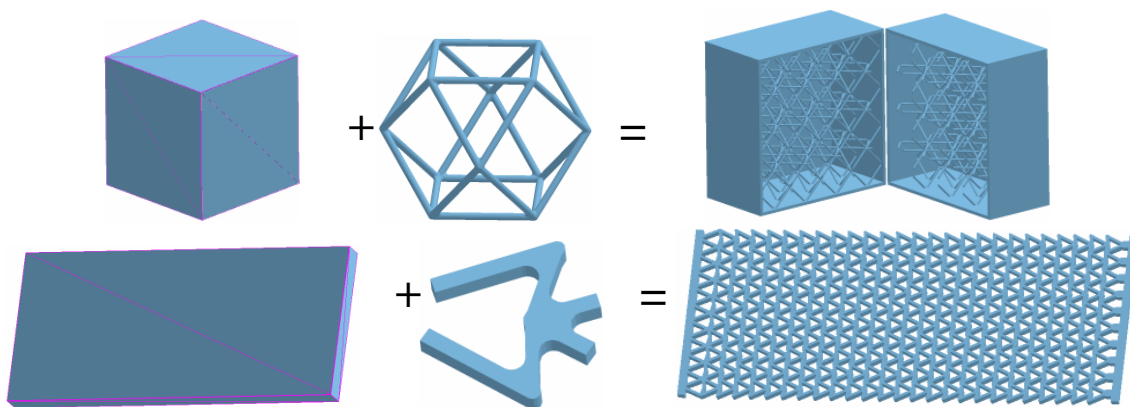
Fig. 3: Two examples of applying mesostructures in a component design [7, 9].

Instead of applying a single mesostructure inside a component such as the two examples shown in Figure 3, we can use various mesostructures at different locations to achieve heterogeneous material properties. That is, for a component G, we can subdivide it into a set of cells C_i such that $G = \bigcup_{i=1}^{n} C_i$. For each cell C_i, we can then map a mesostructure M_i into the cell and use mesostructure boundary connectors B_i to connect M_i with its neighboring mesostructures. Therefore we can generate a new model $G' = \bigcup_{i=1}^{n} (M_i \cup B_i)$. During the above subdivision and mapping processes, we can change the material property at C_i by:

(1) **Using different cell subdivisions**: A component *G* can be subdivided by using different cell sizes and orientations. For example, as shown in [7], we used one or several design requirements to define a warping function *f(V)* and used a space warping technique to minimize an energy function $E(V) = \frac{1}{2} \sum_i \sum_{j \in N_i} f(v_j) \|v_i - v_j\|^2$. Consequently the modified cell subdivision is more adaptive to the given part shape and design requirements.

(2) **Using different mesostructure topology**: As shown in Figure 3, the topology of a microstructure plays a big role in determining its structural properties. Different geometric configurations, such as the strut connectivity, can lead to rigid or flexible behaviors [10].

(3) **Using different mesostructure geometry**: For the same mesostructure orientation and topology, we can also use different design parameter values to generate different geometries. For example, a strut as shown in Figure 3 can have different sizes. Correspondingly, the mesostructures will have different material behaviors.

Therefore, we can use different mesostructures to achieve truly heterogeneous material behaviors even though a rapid manufacturing process such as SLA and SLS provides only a single material such as A6 steel or thermoplastics. Some related work presented the similar idea. Wang [11] presented a unit cell approach for designing lightweight structure and compliant mechanism; Rosen [4] presented a framework for cellular material design for additive manufacturing; and Gupta *et al.* used staggered cell configuration to achieve graded stiffness [12]. Our work is different from the functionally gradient materials (FGM) research for modeling heterogeneous materials for a manufacturing process that can control the material variations in a component [13-15]. However, both types of researches are complimentary. That is, the structural variation in addition to the material variation will enable us to achieve a wide range of material properties.

Our research focuses on how to use controlled structural variation to achieve desired material properties. We first define a *performance-tailored mesostructure* based on the object-oriented programming (OOP) methodology. The OOP is a programming paradigm that uses "objects" and their interactions to design software systems. Currently it is commonly used in the software development. The OOP paradigm enables an object (data and functions) to be reused. The basic pillars of the OOP that are closely related to our application include *encapsulation*, *data hiding*, and *polymorphism*. *Encapsulation* refers to the property of being a self-contained unit. *Data hiding* refers to the ability of using any object without the user knowing or caring about how it works internally. *Polymorphism* refers to the ability of objects belonging to different data types while respond to same method calls.

Fig. 4: An example of a performance-tailored mesostructure that is used to generate the CAD model as shown in Figure 1.

Similar to an object as defined in the OOP, a *performance-tailored mesostructure* consists of four key components: (1) structural configuration (topology), (2) design parameters (geometry), (3) defined boundary, and (4) functional performance. They are explained in more details by using a mesostructure example as shown in Figure 4, which is used to generate the CAD model as shown in Figure 1.

(1) Structural configuration: The topology of a mesostructure plays a big role in determining its structural properties. The researches in material design have developed a lot of structural configurations for different design purposes. For example, Larsen *et al.* [16] developed a structure that possesses the unusual property of having a negative Poisson's ratio. A mesostructure can also integrate very dissimilar physical principles. For example, the mesostructure as shown in Figure 4 mainly uses strut's stretch and compress in *Y* and *Z* axes while it mainly uses strut's bending in *X* axis. In addition to structural properties, other properties such as thermal or acoustic properties can also be used to determine the structural configurations. We use a general definition scheme to define a structural configuration and represent a mesostructure in a *XML* file [9].

(2) Design parameters: A structural configuration and corresponding physical principles give us a range of performance that the mesostructure can achieve. For a desired performance within the range, we can change design parameter values to tailor its geometry for achieving it. If the parametric design approach is used to define a mesostructure, we

can easily change its geometry by modifying the design parameters. For example, the mesostructure as shown in Figure 4 are defined by a set of design parameters such as R_Y, R_Z and r_{Spring}. By changing their values, we can generate a mesostructure to achieve a desired property within its property range.

(3) Structural boundary: Each mesostructure has a set of defined boundaries. They are the interface between neighboring mesostructures. As shown in Section 4, a CAD model synthesizer can automatically integrate all the mesostructures in a component into a valid CAD model. The synthesizer only needs to know the mesostructures' boundaries. The inside geometry of a mesostructure can be hidden. Further, if we define a set of standard boundary, we can change the internal mesostructure geometries without affecting their connections. Therefore we can use different elements to replace a strut. An example is shown in Figure 10.

(4) Functional performance: The mesostructure's performance model is intended to describe its functionality. It includes a set of performance ranges and related functions. A performance range is related to the structural configuration, material property and manufacturing process that will be used to fabricate the mesostructures. For example, a rapid manufacturing process has its limitation on the minimum feature size. Therefore, each design parameter can only have a feasible range in order for the mesostructure to be manufacturable. Correspondingly, the mesostructure will have a limited performance range. A performance function based on the design parameters can be in any forms such as an analytical function, a predefined finite element analysis program, a set of experimental data, or as simple as a prior analysis result. It also needs to consider the dominant physical principles. For example, for the spring in X axis, we need to consider both axis forces and bending moments. We may also have multiple performance functions. For example, for the mesostructure as shown in Figure 4, we will have three different performance functions corresponding to the three axes respectively. Similar to using an object in the OOP, a designer only needs to know the mesostructure's performance in each axis. Its internal structures and related physical principles for achieving the performance can be hidden from the designer. As discussed in the next section, we can build a mesostructure library and find a matching mesostructure based on the desired performance.

3. BUILDING MESOSTRUCTURE'S FUNCTIONAL PERFORMANCE MODEL

In this section, we illustrate the approach of building the functional performance model of a performance-tailored mesostructure. It further demonstrates the key ideas that are presented in Section 2. We use a diaphragm flexure design [17] as the structural configuration of a mesostructure. This also demonstrates that a mesostructure can have a much more complex configuration than a popularly used polyhedron. The 3D view and top view of the defined mesostructure are shown in Figure 5. The central section of the mesostructure is a solid plate. Its outskirts are four uniformly distributed sub-structures which enable the solid plate to have a relatively large deformation when an external force is exerted on the plate. We build a parametric design model of the structure. The important design parameters are marked as $A\sim G$ as shown in Figure 5-right. For the same external force, we can change these parameters to generate mesostructures that can achieve different central displacements.
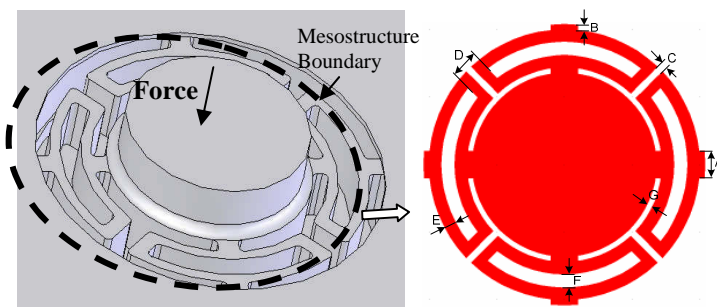
Fig. 5: A mesostructure and its design parameters based on a diaphragm flexure design [17].
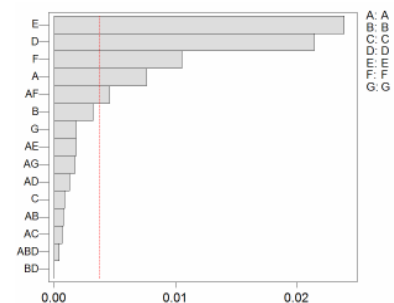
Fig. 6: Pareto chart of the parameter effect related to the central displacement.

Suppose the central displacement is the design performance that a designer is interested in (e.g. for the customized cushion design). We use a finite element analysis software system (*COMSOL*) to quantify the relation between the design parameters and the central displacement. Suppose we will use a SLS machine with *DuraForm* PA plastic, both from *3D Systems Inc.* (www.3dsystems.com), to fabricate the CAD model. The material properties of *DuraForm* PA are used in the FEA simulation. Among the parameter $A\sim G$, we first design a set of experiments to find out the most

significant design variables related to the desired performance. A fractional factorial design based on 7 factors is generated. Accordingly, 16 FEA experiments are performed for the central displacement. An experimental analysis software system (*MINITAB*) is used to analyze the experimental results. The Pareto chart of the parameter effect is shown in Figure 6. Based on the experimental analysis, the most significant factors that contribute to the central displacement are E, D, and F.

Accordingly we fix the design parameters (A, B, C, and G), and design another set of experiments with only the significant design parameters (E, D, and F). A total of 120 FEA analyses are performed. Based on the analysis results, we use *MINITAB* to generate a quadratic regression model between the central displacement and the design parameters. The estimated response surface model is shown as follows.

$Central\_Disp(D, E, F)$ = 0.1563 - 1.4691E + 0.0450F -0.2301D + 5.2845E*E + 0.1223D*D + 1.0261E*D.

We use the original FEA analysis results to verify the generated regression model. We also perform additional FEA analysis to verify the generated regression model. The differences between FEA simulations and the data calculated by the quadratic regression model are within 5%. Therefore, the regression model is validated. For a structure with specified design parameters $A \sim G$, we can then use the regression model to directly estimate the central displacement. This will significantly improve the performance of the optimization process in finding a geometric configuration for a desired central displacement.
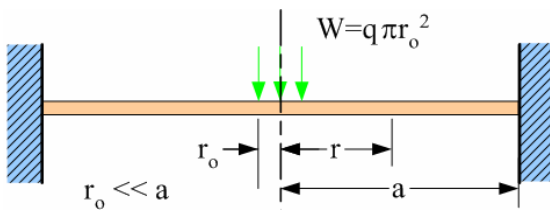
Fig. 7: A clamped circular plate under distributed body force [18].
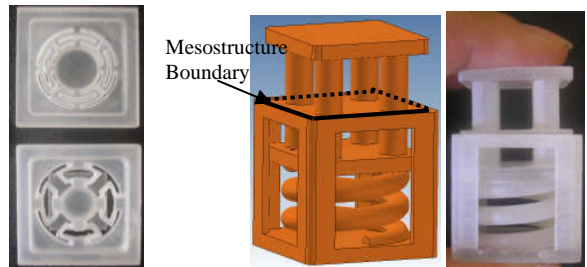
Fig. 8: (left) A photo of the built mesostructure with two sets of parameter values; (right) a mesostructure with spring design that can achieve a bigger central displacement than the mesostructure as shown in Figure 5.

To simplify the material selection, we can also calculate the mesostructure's equivalent material property. Suppose a designer would like to match the Young's Module E in a small region. For a circular plate with fixed supports around its outer boundary (refer to Figure 7), the central displacement of a clamped circular plate under distributed body force can be expressed as: $Central\_Disp = \dfrac{3(1-v^2)qa^4}{4Et^3}$ [18], where q is the distributed loading pressure, t is the thickness, and v is the Poisson ratio. Therefore, the Young's Module of the plate is: $E = \dfrac{3(1-v^2)qa^4}{4 \bullet Central\_Disp \bullet t^3}$. Applying it in our mesostructure, we can calculate the equivalent E value from the central displacement of a geometric configuration ($A \sim G$) by $E_{equivalent} = \dfrac{3(1-v^2)qa^4}{4Central\_Disp(D,E,F) \bullet t^3}$.

In our customized cushion design example, we can use $E_{equivalent}$ value to evaluate the material property at a small region. For a target $E_{equivalent}$ value, we can identify design parameters based on the equation and accordingly generate a mesostructure. For example, a photo of the built mesostructures with two sets of parameter values is shown in Figure 8 (left). Notice each design parameter can only vary within a limited range due to the topological and manufacturing constraints of the mesostructure. Therefore the mesostructure can only achieve a limited range of central displacement. Correspondingly the mesostructure has a limited range of $E_{equivalent}$ values.

If a target $E_{equivalent}$ value is out of the range [$E_{equivalent\_min}$, $E_{equivalent\_max}$] of a mesostructure, we need to use another type of mesostructure in the region. For example, in order to achieve a much smaller $E_{equivalent}$ value (i.e. to generate a much bigger central displacement), we can use a mesostructure as shown in Figure 8 (right) which utilizes simple spring design. Similar to the diaphragm mesostructure, we can identify its design parameters, structural boundary and build a

$E_{equivalent}$ model. A photo of the built spring mesostructure is shown in Figure 8 (right). A simple test verifies that the spring mesostructure can indeed achieve a much bigger central displacement for the same force. Consequently it has a different range of $E_{equivalent}$ values. Another type of element based on staggered cells was presented in [12], which has a different $E_{equivalent}$ model. Therefore, we can build a mesostructure library to have a wide range of $E_{equivalent}$ values. A designer can choose from them for better design performance. The library is reusable and scalable. As shown in Section 4, a *mesostructure selector* can also be developed to aid the designer to select an appropriate mesostructure from the library. In mechanical design, Ashby [19] developed a property cross-plot approach to quantify property-performance relations for the purpose of material selection. We can generate a similar chart based on the $E_{equivalent}$ range for a mesostructure and a rapid manufacturing process. The chart can then be used by the designer in mesostructure selection (refer to Figure 9). Notice the range of performance that can be achieved by the mesostructures can be significantly expanded than that of the solid material.

We can further extend the idea of performance-tailored mesostructure to the level of its element. That is, for each strut of a mesostructure, we can also use an element that has similar boundary to replace it. Therefore, the strut can achieve a wider range of performance. An example is shown in Figure 10. For a strut S_1, we can use a spring element $S_{1'}$ to replace it. Consequently, related boundary B_1 and B_2 are replaced by B_1' and B_2'. This multi-level structural design gives us a tremendous capability in achieving a wide range of desired design performance.
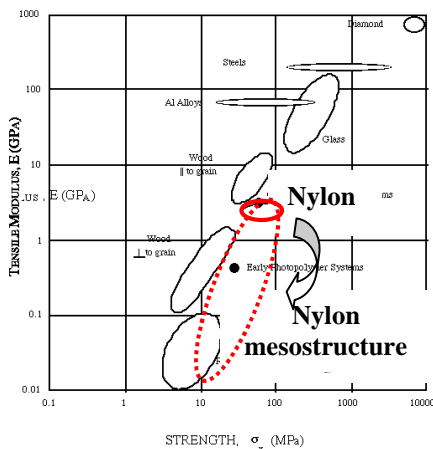
Fig. 9: An illustrative example of applying Ashby chart for the mesostructure selection.
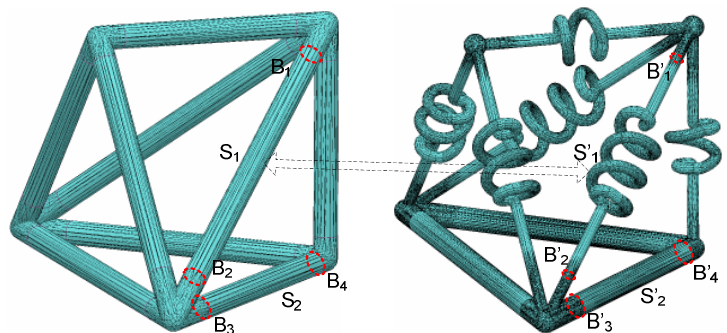
Fig. 10: An illustrative example of applying the idea of performance-tailored mesostructure to its element level.

4. DESIGN FRAMEWORK BASED ON PERFORMANCE-TAILORED MESOSTRUCTURES

Layer-based rapid manufacturing processes enable us to fabricate objects with complex geometry; correspondingly, we can develop a CAD system to model complex geometry. However, the unlimited design freedom poses significant challenges to the finite element analysis (FEA), design optimization tools, and general design methodology. For models as shown in Figure 3, the complexity of the FEA increases sharply as the number of mesostructures increases in the component. Similarly, the design optimization tools need to explore a huge design space which is formed by thousands of mesostructure design variables. More importantly, a design method is required for integrating all the tools into a CAD system that can be easily used by the designers.

Extensive researches in a related field, topology optimization, have studied how to distribute materials in a design domain such that an objective function is extremized. Some popular approaches such as homogenization method [20], ground structure [21], and level set method [13] have been proposed. Most work focuses on 2-dimensional cases mainly due to the extensive computational requirements. In comparison, a performance-tailored mesostructure is a level higher than the element used in topology optimization. That is, hundreds or even thousands of cells marked as "black/white" in topology optimization can form a mesostructure as shown in this paper. Therefore, we believe the performance-tailored mesostructure is a bridge between the system level component design and the micro/meso level material design based on topology optimization.

In this section, we try to address the synthesis of the performance-tailored mesostructures for given design requirements of a product component. In material science and engineering, Olson [22] proposed a three-link chain model as a

general framework for material design (refer to Figure 11-left). Rosen [4] adopted the model and proposed a framework for design for additive manufacturing (DFAM) (refer to Figure 11-right). As shown in the figures, the structure offers a resonant bond between the deductive cause-and-effect logic of science (flows to the right) and the inductive goal-means relations of engineering (flow to the left). We adopt the Process-Structure-Property-Behavior mapping model [4] and present a design framework for component design based on the performance-tailored mesostructures.
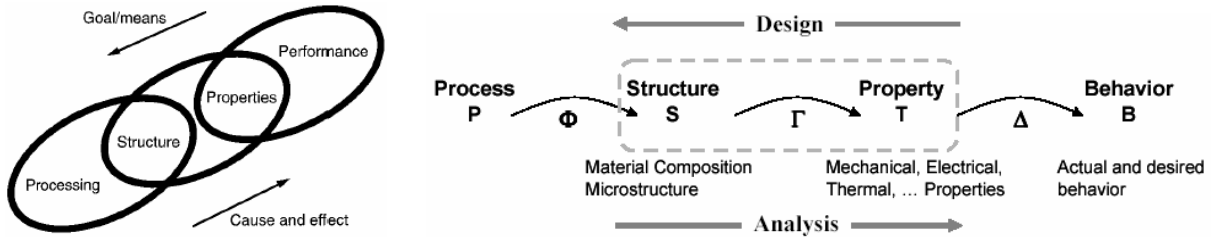
Fig. 11: Systematic design framework: (left) three-link chain model for materials science and engineering [22]; (right) Process-Structure-Property-Behavior model for design for additive manufacturing [4].

As shown in Figure 12, our design framework consists of four design phases.

Phase 1. Component Design. Parametric design optimization in product component level is well studied. It can be defined as a formulation as shown in Tab. 1 (left). A designer selects a material for the component and identifies its material properties such as Young's modulus E from a material handbook. The E value is then treated as a given constant in the FEA tool and design optimizer. The optimization procedure consists of solving a sequence of finite-element problems followed by changing the component's geometry until the optimization process reaches a convergence. In comparison, instead of using the same E value for all the discretized elements, we treat the material property at each element as a design variable. The formulation of the component design based on the performance-tailored mesostructures is shown in Tab. 1 (right).

Parametric design optimization	*Component design based on performance-tailored mesostructure*
<u>Given:</u> **Material property**, loads and constraints	<u>Given:</u> Loads and constraints
<u>Find:</u> Geometric parameters of the part	<u>Find:</u> Geometric parameters and **material property** of the part
<u>Satisfy:</u> Design constraints on design space and boundary conditions	<u>Satisfy:</u> Design constraints on design space and boundary conditions
<u>Bounds:</u> On design variables and performance	<u>Bounds:</u> On design variables and performance
<u>Minimize:</u> Some effective design performance	<u>Minimize:</u> Some effective design performance

Tab. 1: Formulations of design optimization problem.

The key difference between the two formulations is that we use an equivalent material property in each element as a design variable (such as $E_{equivalent}$ as shown in Section 3). Therefore the overall design performance can be improved by utilizing the extra design freedom in the optimization module. We are extending available FEA tool to consider different material property in each element. That is, we can keep track of $E_{equivalent}$ value at each element and use it in assembling a global matrix for analysis. Consequently at each step of optimization procedure, we can determine the equivalent material property for each element. After converging, the generated result includes desired equivalent material property in each element. A designer can also directly specify the desired equivalent material property or modify the optimization result interactively.

Comparing our approach to topology optimization [20], we can discretize the design domain into much larger finite elements. Therefore the complexity of analysis and optimization is greatly reduced. In addition, topology optimization approaches such as homogenization method and simple isotropic material with penalization (SIMP) requires a penalization factor to force the continuous design variables toward a black and white (0/1) solution. Related problems include regions of alternating solid and void elements, referred to as check boards, in the optimal solutions. Also there

is a strong mesh-dependency in the optimal solution such that topologically different solutions appear when the mesh is changed or refined. These problems are all due to the forceful binary design. In our approach, the equivalent material property is treated as continuous variables. There is no forceful binary conversion. In Phase 2 and 3, we can use mesostructure design to achieve the equivalent material property.
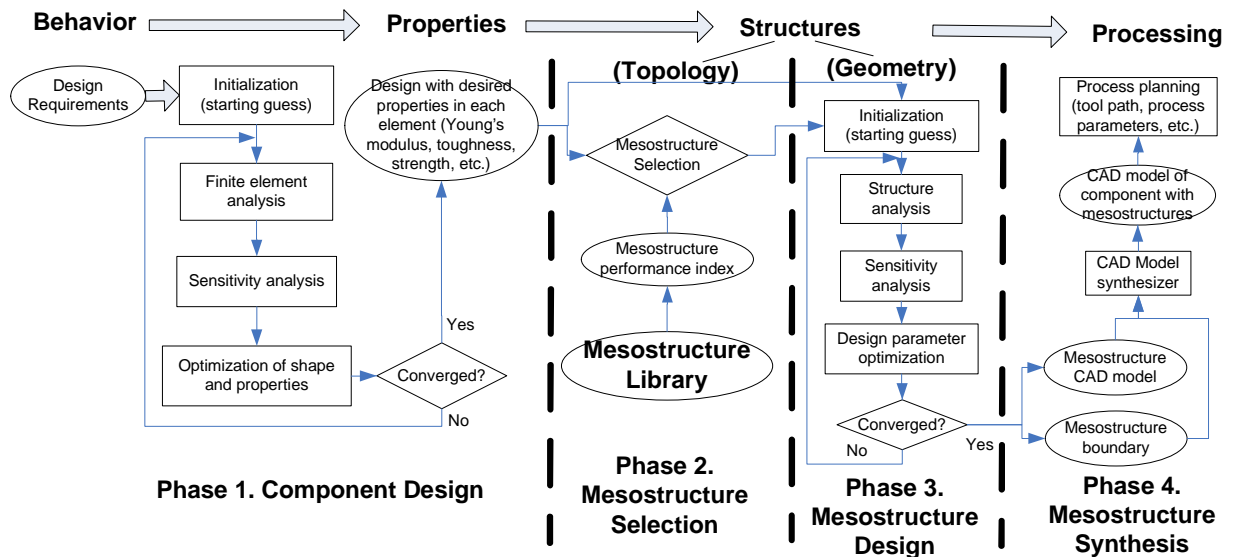
Fig. 12: A design framework based on the performance-tailored mesostructures.

Phase 2: Mesostructure selection. Designing a mesostructure needs to consider its topology and geometry. We divide the mesostructure design into two phases and use two different approaches for them. This is also different from topology optimization approaches in which both structural topology and geometry are treated as design variables. Therefore the optimization problem is quite challenging since it consists both discrete and continuous variables. In our framework, we determine the structural topology by selecting it from a mesostructure library. For a selected mesostructure, we then determine its geometry by parametric design optimization. Therefore, the design optimization process for a selected mesostructure is much simpler with only continuous design variables.

Based on the desired equivalent material property (such as $E_{equivalent}$) in each element, we can select a mesostructure from a library of pre-defined mesostructures by comparing $E_{equivalent}$ with their performance range. We can also consider other factors such as design robustness due to manufacturing defects. As discussed in Section 3, various mesostructures may be selected for a component.

Phase 3: Mesostructure design. For each selected mesostructure, we can further tailor its design parameters to achieve a performance that matches the desired material property in a region. Based on the performance models of a pre-defined mesostructure, we can formulate a parametric optimization problem to find an optimized geometric setting. We can further design a strut element (both topology and geometry) to achieve a desired material property in each strut (refer to the example as show in Figure 10).

Phase 4: Mesostructure synthesis. Each mesostructure has a pre-defined boundary. After mesostructures are selected and tailored for each region, we can gather the boundaries of all the mesostructures. Their connections can be identified based on a standard boundary definition. Therefore, we can automate the synthesis of all the mesostructures and generate a valid CAD model. The CAD model can then be sent to a rapid manufacturing machine for building physical models.

Our design framework is hierarchical. It utilizes a hierarchy of design models that include the component level, the mesostructure level, and the mesostructure's element level. In the component design level, the objectives of material properties are deduced from property-performance relations. Once they are determined, the properties serve as the targets for mesostructure design and further to mesostructure's element design. Therefore our method directly corresponds to the general axiomatic design method developed by Suh [23]. It can also be extended to other properties such as thermal, chemical, and biological properties, in addition to the discussed structural properties.
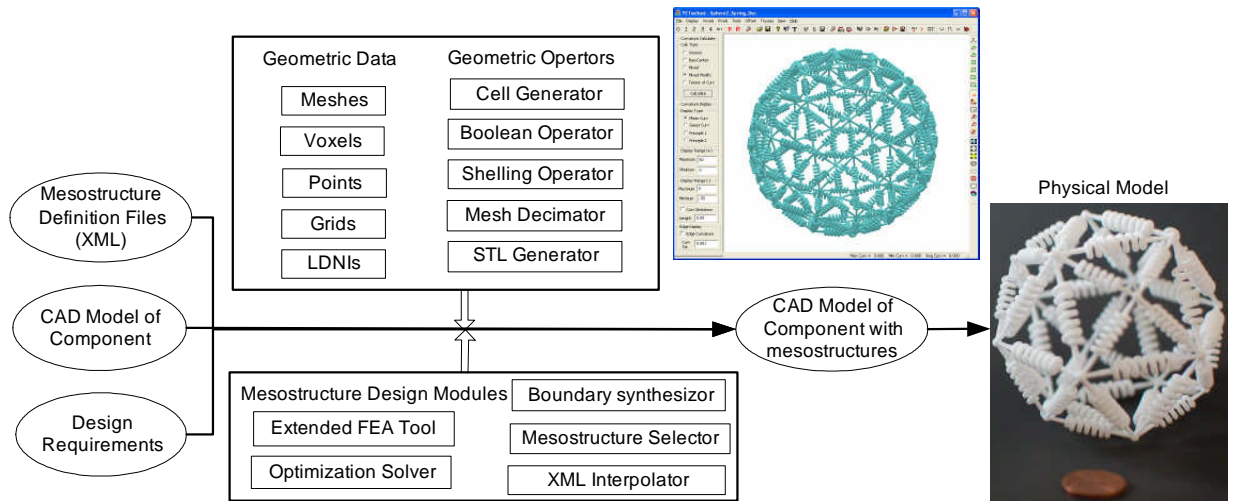
Fig. 13: A CAD system for component design based on performance-tailored mesostructure.

5. A CAD SYSTEM WITH PERFORMANCE-TAILORED MESOSTRUCTURES AND EXAMPLES

We are developing a CAD system independent of any commercial CAD software package. The CAD tool can be used in the component design with the performance-tailored mesostructures (refer to Figure 13-left). A designer can use the CAD system to generate a CAD model (in *STL* format) with mesostructures for rapid manufacturing processes. In the system, we define a mesostructure in XML file according to a standard definition scheme. Currently our mesostructure library has more than 10 different mesostructures. A new mesostructure can be easily added to our system by following the same definition scheme. We utilize multiple geometric data structures in our system for manipulating the geometries of a component and mesostructures. The geometric data structures include boundary meshes (for input and output), voxels/cells (for volumetric analysis), points (for Boolean and shelling), grids (for STL generation), and LDNIs (for Boolean operation). Different data structures are appropriate for different tasks. The mesostructure design modules of the system include an extended FEA tool and an optimization solver (for phase 1 and 3), a XML interpolator and a mesostructure selector (for phase 2), and a boundary synthesizer (for phase 4). A testbed that integrates all the design modules is being developed. A screen capture of the user interface of our testbed with a designed CAD model is shown in Figure 13 (center). A photo of a physical model that was built by the SLS system is shown in Figure 13 (right). The model has performance-tailored spring elements. Consequently, it has certain degree of flexibility. For a big deformation, the bending of the spring elements is obvious. Therefore, the bending analysis needs to be considered in building the performance model for the mesostructure.

We give two examples generated by our testbed to illustrate its capabilities. In Figure 14, the top surface of a chair (marked in orange) is the surface to achieve different rigidity. We first subdivide the surface into a set of small cells. For a mesostructure as shown in Figure 5, we calculate the parameter values (i.e. parameters $A \sim G$ in Figure 5) to achieve a desired rigidity. We then apply the generated mesostructures in all the cells. Therefore, the generated CAD model will have heterogeneous rigidity on the top surface. Notice in the figure, we did not apply the mesostructures to cover the whole surface since the generated STL model is easily over 100MB for a fine sampling. The big file size problem can be mitigated by using a mesh decimator. In Figure 15, we first convert a bunny mesh into a structural model. We then replace a portion of the struts with different sizes of springs. The designed model was successfully built by using a SLS machine with *Duramform* PA. We notice some springs are fragile. We are exploring a better range of the design parameters for the SLS process.

6. CONCLUSIONS AND FUTURE WORK

Typically, mechanical designers choose from a toolbox of materials that have already been developed by material scientists. In this paper, we propose performance-tailored mesostructures which can change or adapt the performance according to the given design requirements. Therefore, the designer will have much more flexibility and capability to design a component with better functions. We define a mesostructure based on the object oriented programming

paradigm to encapsulate the discipline-specific performance models. We then propose a progressive reduction method to integrate the performance-tailored mesostructure with component-level functional models. The designed component can achieve truly heterogeneous properties. We develop a CAD system which incorporates the proposed design framework. The testbed of the CAD system can generate water-tight STL models for layer manufacturing systems. We present several examples to demonstrate the effectiveness of our method.

Our future work includes: (1) we are investigating an effective approach for analyzing the synthesized mesostructures in a component. It is quite challenging to simulate the mechanical properties of a large part with thousands of mesostructures; (2) we would also like to quantify the limitations of rapid manufacturing processes such as the SLS process on the mesostructure design; (3) we are continuing the development of a fully functional CAD system based on the performance-tailored mesostructures.
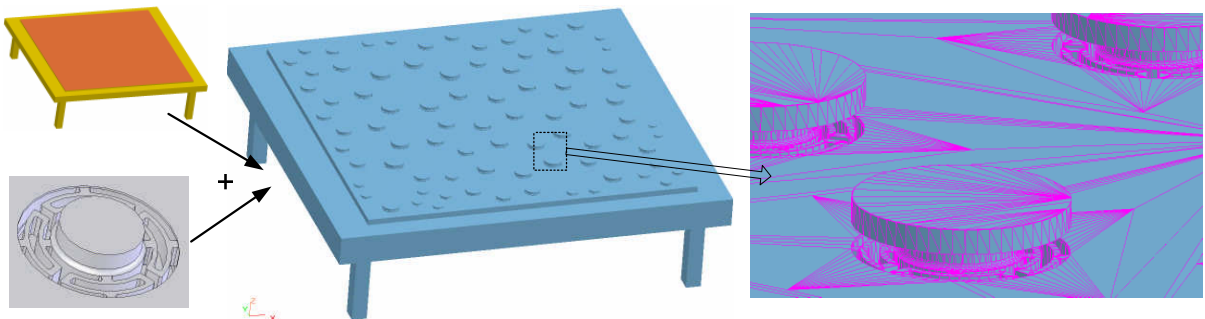
Fig. 14: A chair example with performance-tailored mesostructures.
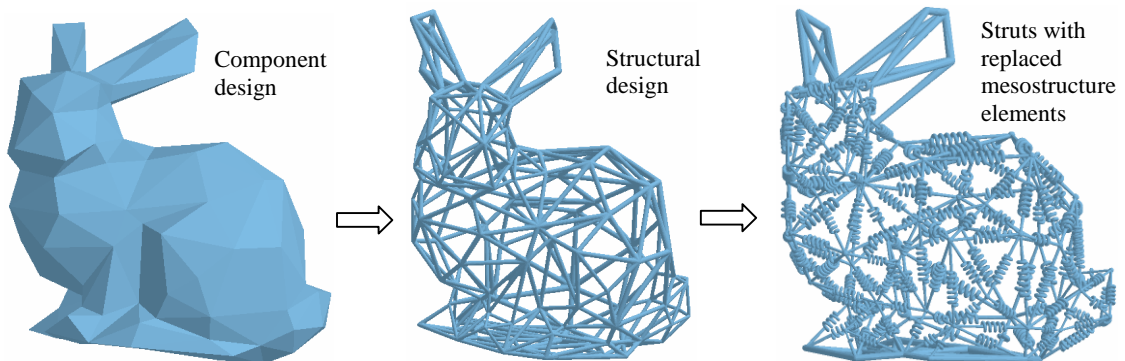
Fig. 15: A bunny example with performance-tailored mesostructures.

7. ACKNOWLEDGEMETS

8. REFERENCES
[1]   Bedsore: http://en.wikipedia.org/wiki/Pressure_sore, Wikipedia.
[2]   Cushmaker: http://www.cushmaker.com.
[3]   Hopkinson, N.; Hague, R.; Dickens, P.: Rapid Manufacturing: An Industrial Revolution for the Digital Age, John Wiley & Sons, 2006.
[4]   Rosen, D. W.: Computer-aided Design for Additive Manufacturing of Cellular Structures, Computer-Aided Design and Application, 4(5), 2007, 585-594.

[5]   Deshpande, V. S.; Fleck, N. A.; Ashby, M. F.: Effective properties of the octet-truss lattice material, Journal of the Mechanics and Physics of Solids, 49, 2001, 1747-1769.

[6]   Chiras, S.; Mumm, D. R.; Evans, A. G.; Wicks, N.; Hutchinson, J. W.; Dharmasena, K.; Wadley, H. N. G.; Fichter S.: The Structural Performance of Near-optimized Truss Core Panels, International Journal of Solids and Structures, 39, 2002, 4093-4115.

[7]   Chen, Y.: 3D Texture Mapping for Rapid Manufacturing, Computer-aided Design and Application, 4(6), 761-771, 2007.

[8]   Sigmund, O.: A New Class of Extremal Composites, Journal of Mechanics and Physics of Solids, 48, 2000, 397-428.

[9]   Chen, Y.: A Mesh-based Geometric Modeling Method for General Structures. ASME International Design Engineering Technical Conferences and Computers and Information in Engineering Conferences, Philadelphia, PA, September 10-13, 2006, DETC2006-99513.

[10]   Deshpande, V. S.; Ashby, M. F.; Fleck, N. A.: Foam Topology: Bending versus Stretching Dominated Architectures, Acta Materialia, 49(6), 2001, 1035-1040.

[11]   Wang, H.: A Unit Cell Approach for Lightweight Structure and Compliant Mechanism, Ph.D. Thesis, Georgia Institute of Technology, Atlanta, GA, 2005.

[12]   Gupta, G.; Tan, J.; Seepersad, C.C.: Design and Freeform Fabrication of Compiliant Cellular Materials with Graded Stiffness, Proceedings of the Solid Freeform Fabrication Symposium, Austin, TX, 2006.

[13]   Wang, M. Y; Wang, X.: A Level-set based Variational Method for Design and Optimization of Heterogeneous Objects, Computer-Aided Design, 37(3), 2005, 321-337.

[14]   Qian, X.; Dutta, D.: Feature based Design for Heterogeneous Objects, Computer-Aided Design, 36(12), 1263-1278, 2004.

[15]   Jackson, T. R.: Analysis of Functionally Graded Material Object Representation Methods, Ph.D. Thesis, Massachusetts Institute of Technology, Boston, MA, 2000.

[16]   Larsen, U. D.; Sigmund, O.; Bouwstra, S.: Design and Fabrication of Compliant Mechanisms and Material Structures with Negative Poisson's Ratio, Journal of Microelectromecahnical Systems, 6(2), 1997, 99-106.

[17]   Awtar, S.: Constraint-based Design of Flexure Mechanisms, ASME International Design Engineering Technical Conferences and Computers and Information in Engineering Conferences, Las Vegas, NV, September 4, 2007, Tutorial #5.

[18]   Young, W.: Roark's Formulas for Stress and Strain, Mcgraw-Hill, 6th edition, 1989.

[19]   Ashby, M.: Materials Selection in Mechanical Design, Butterworth-Heinemann, 2nd Ed, 1999.

[20]   Bendsoe, M. P.; Sigmund, O.: Topology Optimization: Theory, Methods and Applications, Springer, 2nd Ed., 2003.

[21]   Joo, J.; Kota, S.; Kikuchi, N.: Topological Synthesis of Compliant Mechanisms Using Linear Beam Elements, Mechanics of Structures and Machines, 28(4), 2000, 245-280.

[22]   Olson, G. B.: Computational Design of Hierarchically Structured Materials, Science, 277(29), 1997, 1237-1242.

[23]   Suh, N. P.: The Principles of Design, Oxford University Press, New York, 1990.